Comparison of Simulation Results for an Office Building Between Different BES Tools

The Challenge of Getting Rid of Modeller Influence and Identifying Reasons for Deviations

Magni, Mara; Ochs, Fabian; Bonato, Paolo; D'Antoni, Matteo; Geisler-Moroder, David; de Vries, Samuel; Loonen, Roel; Maccarini, Alessandro; Afshari, Alireza; Calabrese, Toni

Published in:
Proceedings of Building Simulation 2019

DOI (link to publication from Publisher):
10.26868/25222708.2019.210834

Publication date:
2019

Document Version
Publisher's PDF, also known as Version of record

BS 2019 2-4 SEPT ROME 16th IBPSA INTERNATIONAL CONFERENCE AND EXHIBITION

INTERNATIONAL BUILDING PERFORMANCE SIMULATION ASSOCIATION

Comparison of Simulation Results for an Office Building Between Different BES Tools – The Challenge of Getting Rid of Modeller Influence and Identifying Reasons for Deviations

Mara Magni[1], Fabian Ochs[1], Paolo Bonato[2], Matteo D'Antoni[2], David Geisler-Moroder[3], Samuel de Vries[4], Roel Loonen[4], Alessandro Maccarini[5], Alireza Afshari[5], Toni Calabrese[1]
1 University of Innsbruck, Unit for Energy Efficient Buildings, Innsbruck (Austria)
2 Eurac Research, Institute for Renewable Energy, Bolzano (Italy)
3 Bartenbach GmbH, Aldrans (Austria)
4 Eindhoven University of Technology, Eindhoven (The Netherlands)
5 Aalborg University Copenhagen (Denmark)

Abstract

The model of the reference office building, reported in IEA SHC Task 56, is implemented by different experts in building simulations, with different tools (i.e. dynamics simulation tools such as EnergyPlus, TRNSYS, CarnotUIBK, ALMAbuild, DALEC, Modelica and quasi steady state calculation tool such as PHPP). The aim is to set up reference models for (virtually) testing different solar passive and solar active façade systems. Hence, identifying deviations between the resulting energy balance for heating and cooling of the used tools due to different levels of detail of their models is of great importance, while in the same time, trying to get rid of the user influence was experienced as a real challenge.

It can be concluded that even considering a relatively simple case study, it is hard to reach a good agreement between different tools and an additional calibration phase is necessary. In particular, it was found that the resolution of the window model can lead to considerable differences.

As a perspective, it seems to be a challenge if the building modelling is entrusted to non-expert users (e.g. from Building Information Modelling to Building Energy Modelling, where BIM-to-BEM interoperability issues might arise and affect the simulation results).

Introduction

In spite of higher efficiency, the energy consumption of buildings has increased over the past decades and currently accounts for approximately 37% of the total primary energy consumption in European Union (i.e. 26% is taken up by residential and 11% by commercial buildings) (Pérez-Lombard, et al., 2008). The European Union has set three key targets for the year 2030: 40% cuts in greenhouse gas emissions, 27% share for renewable energy, 27% improvement in energy efficiency (Council of the European Union, 2014). To reach this goal, the building system will be required to be an energy producer other than an energy consumer (i.e. prosumers) (Brange, et al., 2016). Nowadays, solar thermal systems for building integration are gaining attention. Advanced materials and technologies are integrated into the building envelope with the aim to reduce the energy needs (energy conservation) or to collect energy from local sources reducing the primary energy consumption (energy collection) (Martinez, et al., 2017). The use of dynamic simulations can play an important role in helping designers and researchers to analyse the integration of renewables, the improvement of the efficiency and the reduction of the demand of the system. However, conclusions from simulation studies can be influenced by the calculation algorithms, numerical errors, non-identical inputs, different processing of climate data and on the choice of physical model (Feist, 1994).

The scientific community contributed to the progress of dynamic simulation by proposing different tools and approaches (Castaldo and Pisello, 2018). Studies regarding the comparison between different tools, are present in the literature. Kim, et al., (2013) presented a stochastic calibration and comparison between a simplified calculation approach (ISO 13790:2008, 2008) and EnergyPlus for an office building. The calibrated ISO 13790:2008 delivers results significantly identical to the dynamic model while the non-calibrated fails. Dermentzis, et al., (2019) evaluated an energy auditing tool (PHPP) against TRNSYS for a set of buildings and climates. The results show that the average deviation between the tools is 8% for the heating demand and 15% for the cooling demand. Strachan, et al., (2016) carried out an empirical analysis involving 21 modelling teams with different simulation programmes. After the building validation phase, in which a significant number of input errors were detected, many of the tested programs showed a good agreement with the measured data. Since new tools (e.g. CarnotUIBK, ALMAbuild, DALEC) and updated software versions are available, it is important to continue carrying out new comparison studies, although some are already present in the literature.

Within this scenario, IEA SHC Task 56 Subtask C, (IEA, 2016) describes the boundary conditions to adopt for the transient simulation of a reference office room, that allows each dynamic simulation tool user to implement the same building system. The office cell is representative for a typical new European office space and is taken as a reference for the study of different solar active façades. To ensure the credibility of this reference, it is important that it can be implemented in different BPS tools, and that there is only modest deviation between the results. In this work, the model of the reference office cell, described in D'Antoni, et al., (2017), is developed by experienced users of building simulation software, with different tools

https://doi.org/10.26868/25222708.2019.210834

(i.e. the dynamic simulation tools EnergyPlus, TRNSYS, CarnotUIBK, ALMAbuild, DALEC, Modelica and the quasi steady state calculation tool PHPP). The tools analysed in this work have different focus and depending on it, component models (window, wall, HVAC, control, etc.) vary from simplified to detailed. The results of the different tools are compared considering all the components of the building energy balance. Particular attention is given to the window model because, in this case study, it strongly influences the results.

Methods

Boundary Conditions

The reference building is chosen in order to be representative of a typical European office cell located in middle floor of a high-rise building. Three different European climates are considered in this study: Rome (hot temperate), Stuttgart (cold temperate) and Stockholm (cold climate). Figure 1 shows the considered office cell, which has a heated area of 27 m^2 and a volume of 81 m^3. All the surfaces are considered adiabatic, except for the façade oriented toward South (with window-to-wall ratio of 60%) where ambient boundary conditions are applied and solar active technologies such as daylighting systems can be installed (not applied in the present comparison). Shading from adjacent obstacles is not considered, whereas an external movable shading, able to block 70% of the incoming radiation, is activated when direct solar radiation impinging the south façade is higher than 120 W/m^2.

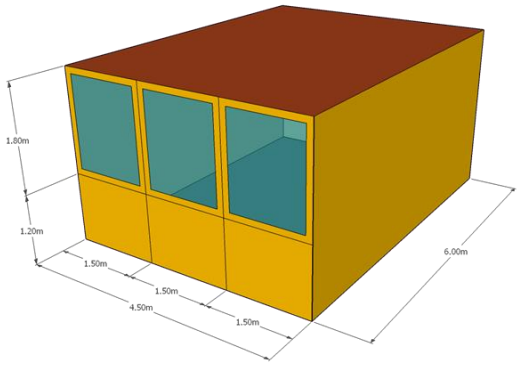

Figure 1: View of the reference office zone.

The thermal properties of the wall infill element and the characteristics of the windows depend on the three climates, as shown in Table 1. The internal walls are typical plasterboard walls, the exterior wall is a three layer structure with different insulation thicknesses depending on the climate.

Table 1: Main properties of the south oriented façade.

Properties	Rome (Italy)	Stuttgart (Germany)	Stockholm (Sweden)
$U_{ext,wall}$ [W/m^2K]	0.80	0.40	0.20
U_{win} [W/m^2K]	1.26	1.35	0.90
g-value [-]	0.33	0.59	0.63
T_{sol} [-]	0.462	0.426	0.260
Rf_{sol} [-]	0.237	0.266	0.218
T_{vis} [-]	0.749	0.706	0.659

Table 2 shows the yearly average ambient temperature ($T_{amb,av}$), yearly global irradiation over a horizontal surface ($I_{g,h}$) and yearly irradiation over a south oriented vertical surface (I_{south}) for each climate.

Table 2: Main boundary conditions: yearly average ambient temperature ($T_{amb,av}$), yearly global irradiation over a horizontal surface ($I_{g,h}$) and yearly irradiation over a south oriented vertical surface (I_{south}).

Location	$T_{amb,av}$ [°C]	$I_{g,h}$ [kWh/m^2]	I_{south} [kWh/m^2]
Rome	15.8	1632	1253
Stuttgart	9.9	1101	889
Stockholm	7.8	952	884

User behaviour (e.g. occupancy, appliances and lighting) is taken into account by means of hourly profiles, different for week and weekend days (SIA, 2015). Figure 2 reports the schedule profiles for occupancy, appliances and lighting. A contemporaneity index of 0.8 is used for occupancy and appliances. Three persons are present during the working time and a sensible and latent heat of 70 W/person and 0.08 kg/h/person are considered. The internal gain due to appliances is assumed to be 7 W/m^2 and the electric gain due to lighting is 10.9 W/m^2.

The lighting schedule follows occupied hours and is defined considering a non daylight responsive system

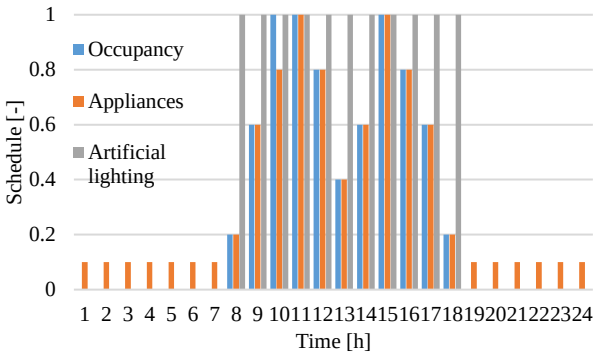

Figure 2: Schedule profile for occupancy, appliances and lighting.

The natural infiltration rate is assumed to be constant and equal to 0.15 1/h. A fresh air supply of 40 m^3/h/person is covered by a mechanical ventilation system with heat recovery (70% sensible efficiency). A bypass of the heat recovery is activated when the temperature of the zone is higher than 23 °C and the ambient temperature is lower than the indoor temperature.

Simplified all-air heating and cooling systems are included within the models. The set point temperature for the indoor convective temperature during the wintertime and summertime are 21 °C and 25 °C. When the convective temperature is between 21 °C and 25 °C neither the cooling system nor the heating system are activated. A detailed description of the boundary conditions is reported in D'Antoni, et al., (2017).

General modelling features

The tools analysed in this work have different focus:

- EnergyPlus™ (EP) is a whole building energy simulation program that engineers, architects, and researchers use to model both energy consumption for heating, cooling, ventilation, lighting and plug and process loads and water use in buildings (Crawley, et al., 2000) ;
- TRNSYS (TRN) is a transient system simulation program based on a component approach with modular structure. The TRNSYS library includes a detailed multizone building model and components for HVAC systems, renewable energy systems, etc. (Klein, et al, 1979);
- Simulink UIBK (SIM_IBK) is a Matlab/Simulink library, compatible with CARNOT Toolbox, developed by the University of Innsbruck, based on object-oriented programming of a parameterized building model (Siegele, et al., 2019);
- ALMAbuild (SIM_BO) is a Matlab/Simulink library, compatible with CARNOT Toolbox, developed by the University of Bologna where a user develops a building model by means of a series of Graphical User Interfaces (Campana, et al., 2017);
- DALEC (DAL) is a free web tool developed by Bartenbach, University of Innsbruck and Zumtobel. The main focus is on combined thermal and lighting building simulations in early design phases (Werner, et al., 2017);
- MODELICA (MOD) is a non-proprietary, object-oriented, equation based language to conveniently model complex physical systems, with a wide open source library (in this case the LBNL Buildings library is used) (Wetter, et al., 2014);
- PHPP Passive House Planning Package is a quasi steady state calculation tool, developed as spread sheet, for the use of architects and planning experts (Feist, 2019).

The different tools implement models with different level of detail and approach the numerical solution of the building system with different equations.

Table 3 reports the physical models used by the different tools for the calculation of the room balance and the time step used in the numerical simulations. The two star node model includes a convective node (representing the thermal capacity of the air) and a radiative node (the long-wave radiative exchange between the surfaces is modelled using the star network). In the simplified calculation mode, TRN implements a star network where an artificial temperature node (Tstar) is used to consider the parallel energy flow from the inside wall surface to the zone air by convection and the long-wave radiation exchange between the surfaces. EP uses a grey interchange model (ScriptF) involving an approximation of direct view factors for the radiative exchange between surfaces.

MOD implements a more detailed model for the radiative exchange based on net radiation exchange approach (Wetter, et al., 2011). DAL model is based on the Standard ISO 13790:2008 where the room heat balance is solved considering three nodes and both the air temperature and mean radiant temperature are calculated. The nodes are connected between each other by means of specific coupling conductance defined by the standard. The whole thermal capacity of walls and air volume is connected to the node representing the mean radiant temperature. PHPP is a quasi steady state tool that calculates losses and gains considering a fixed set point temperature. It performs two different balances by using the two set point temperatures for winter and summer.

Each tool performs the simulation using different time steps and, in particular: SIM_IBK and SIM_BO use variable-step solvers, which vary the step size during the simulation depending on the required numerical accuracy and the solver. All the other tools perform the calculation with a constant time step as reported in Table 3. The definition of the time step influences the run time and the accuracy of the results.

Table 3: Model of the room heat balance and simulation time step.

Tools	Surface to zone heat transfer	Time step
EP	Radiative and conv. node	Const.: 15 m
TRN	Star node model	Const.: 60 m
SIM_IBK	Two star node model	Var.: max 10 m
SIM_BO	Two star node model	Var.: max 10 m
DAL	Standard ISO 13790	Const.: 60 m
MOD	Radiosity and conv. node	Const.: 15 m
PHPP	Steady state balance	Monthly

Table 4 reports the model used for the wall structure in each tool. EP and TRN model the opaque structure with the transfer function method, whereas both Simulink libraries and MOD are based resistance-capacity (R-C) method. DAL and PHPP implement a simplified model of the walls, based on the overall heat transfer coefficient (H) of the external structures.

Table 4: Model of the walls.

Tools	Wall model
EP	Transfer function
TRN	Transfer function
SIM_IBK	R-C
SIM_BO	R-C
DAL	Unique H value
MOD	R-C
PHPP	Unique H value

Different window models are implemented in the analysed tools, (Table 5). In particular, EP, TRN, SIM_BO and MOD perform an energy balance over each pane of the window while DAL, SIM_IBK and PHPP are based on a simplified window thermal model where the transmission losses of the window are calculated by using a constant heat transfer coefficient. An additional layer representing the shading system is involved in the thermal balance of the window only in EP and MOD.

Gains from solar radiation are computed differently in each tool. EP, TRN, SIM_BO and MOD consider how

solar radiation is absorbed by each pane of the window, which increases the pane temperature, and influences convective and radiative exchange.

In the presented heat balances for EP, SIM_BO and MOD solar gains are defined as directly transmitted radiation (convective and radiative gains from the inner pane do contribute to the room heat balance but they are not reported as 'solar gains' in the presented balances). The calculation of the solar gain in DAL is based on an angular dependent g-value of the façade dependent on the sun position, SIM_IBK calculation is based on an angular dependent g-value of the glazing system, dependent on the sun position. Depending on the definition of the solar gain (total or only transmitted part), also the definition of the transmission losses is different. When only the directly transmitted part of the solar radiation is reported as solar gain, the transmission loss is represented by the exchange between the internal side of the window and the thermal zone ($\dot{Q}_{int,p2}$ in Figure 3). Contrariwise, when the total solar gain is reported (including absorbed solar radiation reemitted to the inside), the transmission losses are calculated as ($\dot{Q}_{tr,p1-p2}$ in Figure 3).

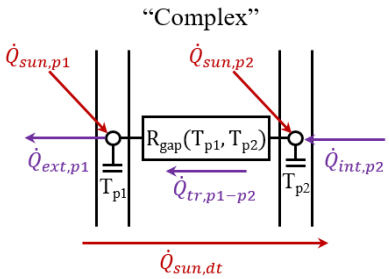

Figure 3: Sketch of the Complex window model.

The models used to predict the diffuse radiation on a tilted surface can be based on either isotropic or anisotropic sky models. All the tools except for DAL calculate the diffuse radiation on a tilted surface with anisotropic sky models while DAL uses an isotropic sky model.

Table 5: Window model.

Tools	Window model	Solar Gain
EP	'Complex'	Directly transmitted (τ-sol)
TRN	'Complex'	Total
SIM_IBK	'Simplified'	Total (g-value)
SIM_BO	'Complex'	Directly transmitted (τ-sol)
DAL	'Simplified'	Total (g-value)
MOD	'Complex'	Directly transmitted (τ-sol)
PHPP	'Simplified'	Total (g-value)

The profiles for the occupancy, appliances and lighting could not be implemented in DAL and PHPP. In DAL a constant internal gain of 8.79 W/m^2 from 8 a.m. to 19 p.m. is considered while in PHPP a constant internal gain of 6.5 W/m^2 is considered.

With regard to the ventilation system, EP, TRN, SIM_IBK, SIM_BO and MOD calculate the ventilation rate, bypass control and infiltration losses as described in the report (D'Antoni, et al., 2017) while DAL uses a constant energy equivalent air exchange rate that takes into account the infiltration and energy effective air exchange rate. The additional ventilation losses due to activation of the bypass are modelled as window/night ventilation. PHPP considers ventilation losses using a constant equivalent air exchange rate. A different rate is used, for summertime and wintertime, which account for the frequency with which the bypass is activated in that period. These equivalent air exchange are calibrated in order to match the ventilation losses calculated by SIM_IBK.

The shading control system is modelled based on a 120 W/m^2 beam direct solar radiation threshold as described in the report (D'Antoni, et al., 2017) for all the tools except for the PHPP where it is only possible to set a constant value for the summer and winter time. The shading values are calibrated in order to match the solar gain calculated by SIM_UIBK.

Table 6: Internal gain profile and ventilation rate.

Tools	Internal Gain	Ventilation rate/control	Shading control
EP	Profile	Profile/Dynamic ctr.	Dynamic
TRN	Profile	Profile/Dynamic ctr.	Dynamic
SIM_IBK	Profile	Profile/Dynamic ctr.	Dynamic
SIM_BO	Profile	Profile/Dynamic ctr.	Dynamic
DAL	Constant	Constant	Dynamic
MOD	Profile	Profile/Dynamic ctr.	Dynamic
PHPP	Constant	Constant	Constant

Simulation Results

Comparison between simulation results

The reference office building is simulated with the different tools considering three different locations (i.e. Rome, Stuttgart and Stockholm, see Table 2. The properties of the wall and windows are varied with the climate (see Table 1). Table 7 shows the yearly simulation results, for each scenario, reporting heating demand Q_h, cooling demand Q_c, sum of ventilation and infiltration losses Q_{vv}, transmission losses Q_{tr} and solar gains Q_{sol}. Internal gains Q_{gi} are not shown because the annual sum is the same for each tool in each instance (i.e. 56.5 kWh/(m^{2}a)).

PHPP outputs only the heating and cooling demand, the other components are estimated starting from the summer and winter balance calculated by the PHPP. The transmission losses and solar gains have to be analysed bearing in mind, the different definitions used by the different tools (see previous section).

The heating demand increases with the colder climates in spite of the higher insulation level of the envelope. The solar gain is higher in Stuttgart and Stockholm compared to Rome because the glazing system has lower g-value (see Table 1) and because of lower solar altitude angles. The presence of a high efficiency heat recovery unit ensures lower ventilation losses.

Table 8 shows the relative deviation of the results reported in Table 7 with respect to the median value. The high relative deviation for the heating demand in Rome is caused by the low absolute values of heating demand. For the cooling demand, which contributes most to the energy demand in all the climates, the deviation between the

different tools reaches the maximum value of 21% in Stockholm.

Table 7: Yearly simulation results for all the cases.

Loc.	Tools	Q_h	Q_c	Q_{vv}	Q_{tr}	Q_{sol}
		[kWh/(m^{2}a)]				
ROME	EP	3.6	-36.4	-27.1	-19.8	25.4
	TRN	3.5	-33.3	-30.6	-29.1	32.9
	SIM_IBK	5.8	-38.2	-30.4	-30.3	36.8
	SIM_BO	3.1	-33.4	-29.5	-23.1	25.9
	DAL	5.9	-35.9	-31.7	-37.7	42.7
	MOD	7.1	-34.0	-31.0	-30.0	31.4
	PHPP	5.7	-37.9	-28.6	-34.1	36.6
	MEDIAN	5.7	-35.9	-30.4	-30.0	32.9
STUTTGART	EP	15.8	-28.1	-42.4	-47.3	48.4
	TRN	18.7	-23.2	-45.8	-66.2	59.9
	SIM_IBK	16.0	-31.7	-47.4	-49.7	56.4
	SIM_BO	13.2	-23.9	-45.1	-37.7	37.1
	DAL	18.2	-28.4	-45.9	-56.2	56.8
	MOD	17.1	-27.9	-49.3	-42.2	45.8
	PHPP	14.5	-27.6	-47.7	-56.5	56.7
	MEDIAN	16.0	-27.9	-45.9	-49.7	56.4
STOCKHOLM	EP	17.0	-32.2	-50.2	-34.2	46.0
	TRN	21.3	-23.8	-50.5	-61.6	58.0
	SIM_IBK	14.5	-31.0	-54.3	-41.9	56.2
	SIM_BO	17.4	-23.6	-49.3	-38.6	37.7
	DAL	16.9	-28.2	-52.7	-44.6	52.8
	MOD	14.5	-30.0	-54.4	-39.3	52.7
	PHPP	14.6	-31.0	-55.1	-44.8	56.2
	MEDIAN	16.9	-30.0	-52.7	-41.9	52.8

Table 8: Relative deviation with respect to the median value.

Loc.	Tools	Q_h	Q_c	Q_{vv}	Q_{tr}	Q_{sol}
ROME	EP	-36%	1%	-11%	-34%	-23%
	TRN	-38%	-7%	1%	-3%	0%
	SIM_IBK	2%	6%	0%	1%	12%
	SIM_BO	-46%	-7%	-3%	-23%	-21%
	DAL	4%	0%	4%	26%	30%
	MOD	25%	-5%	2%	0%	-5%
	PHPP	0%	6%	-6%	14%	11%
STUTTGART	EP	-1%	0%	-8%	-5%	-14%
	TRN	17%	-17%	0%	33%	6%
	SIM_IBK	0%	13%	3%	0%	0%
	SIM_BO	-17%	-15%	-2%	-24%	-34%
	DAL	14%	2%	0%	13%	1%
	MOD	7%	0%	7%	-15%	-19%
	PHPP	-9%	-1%	4%	14%	1%
STOCKHOLM	EP	1%	7%	-5%	-18%	-13%
	TRN	26%	-21%	-4%	47%	10%
	SIM_IBK	-14%	3%	3%	0%	6%
	SIM_BO	3%	-21%	-6%	-8%	-29%
	DAL	0%	-6%	0%	6%	0%
	MOD	-14%	0%	3%	-6%	0%
	PHPP	-13%	3%	5%	7%	6%

A good agreement is reached for the ventilation and infiltration losses, where the relative deviation is lower than 11%. Transmission losses and solar gain have to be analysed considering the different definition of these components used by the different tools (see previous section). Solar gain and transmission losses are expected to be lower or equal to the average for EP, SIM_BO and MOD. SIM_IBK and PHPP have similar ventilation-infiltration losses and solar gain because the average air exchange rate and the effective shading value used in the PHPP were "calibrated" taking as a reference SIM_IBK.

Figure 4 reports the monthly heating and cooling demand for each tool for the climates of Rome, Stuttgart and Stockholm. From March to November in Rome, and from April to October in Stuttgart and Stockholm, the cooling demand is higher than the heating demand. TRN and SIM_BO have the lowest cooling demand in each climate, with deviations with respect to the median values of each month, ranging for the climates of Stockholm from -93% to -1%, for Stuttgart from -85% to +0% and for Rome from -49% to 0%. The results present higher deviation, especially for the cooling demand, during the transition months, when longer periods in which the temperature is free to float are present, while during the central summer month deviations are contained between +15% and -10%. TRN features the highest heating demand during the winter months, with deviations from the monthly median values, ranging from +24% to +36% and +9% to +21%, for the climates of Stockholm and Stuttgart respectively. SIM_BO has the lowest heating demand every month for the climates of Rome and Stuttgart.

Figure 5 shows the monthly average convective temperature. The internal and solar gains cannot be easily dissipated through the well-insulated envelope and therefore, high indoor temperatures also occur during mid-seasons. This can be clearly seen in Figure 5, where all the tools have an average temperature higher than the heating set point also during the coldest month of the coldest climates. In Rome, the heating demand is nearly zero and the convective temperature is higher than the heating set point. Longer periods in which the convective and mean radiant temperatures are not controlled by either the heating system or the cooling system occur during the transition months.

The dynamic behaviour of the free floating temperature is influenced by the way in which the tools model the thermal capacity of the building and the convective and radiative exchange occurring within the studied office cell. DAL models the office zone with only one thermal capacity and this assumption has an influence on the convective average temperature, which is the highest during the winter months. Deviations in convective and mean radiant temperature influence heating and cooling demands. The deviation with respect to the median value for each month (excluding the temperature from PHPP) are within -2% and +3%. The maximum deviation is reached during the transition months. Figure 6 shows the monthly solar irradiation impinging the south façade for every tool in each climate. It can be seen that all tools are in good agreement except for DAL, which presents lower irradiation (in average -15% with respect to the median value). This is due to the different methods used for the calculation of the solar radiation on a tilted surface, all the tools are based on anisotropic model of the sky while DAL models the diffuse part of the sky radiation as isotropic.

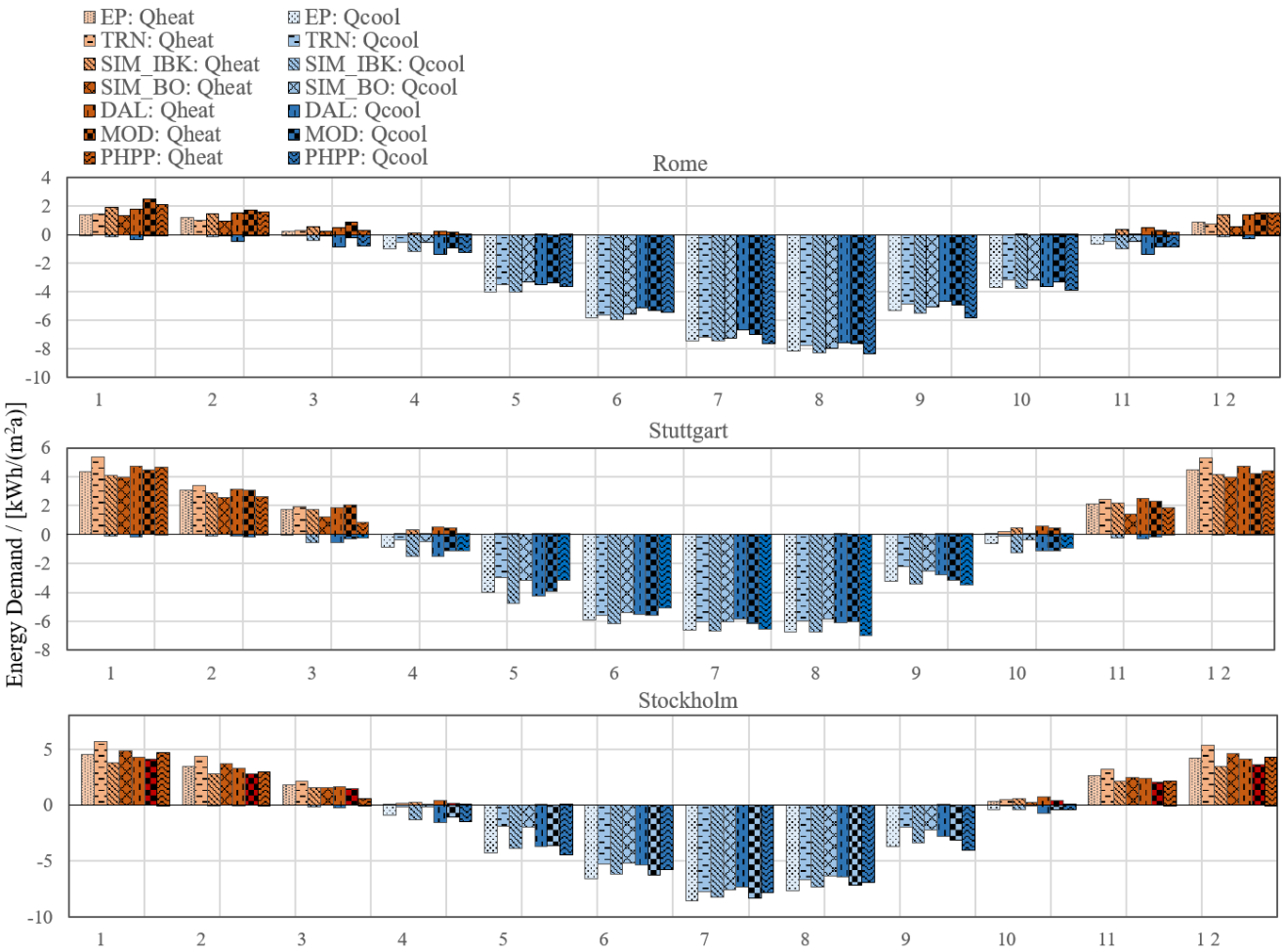

Figure 4: Comparison of monthly heating and cooling demands simulated with all the considered tools and climates.

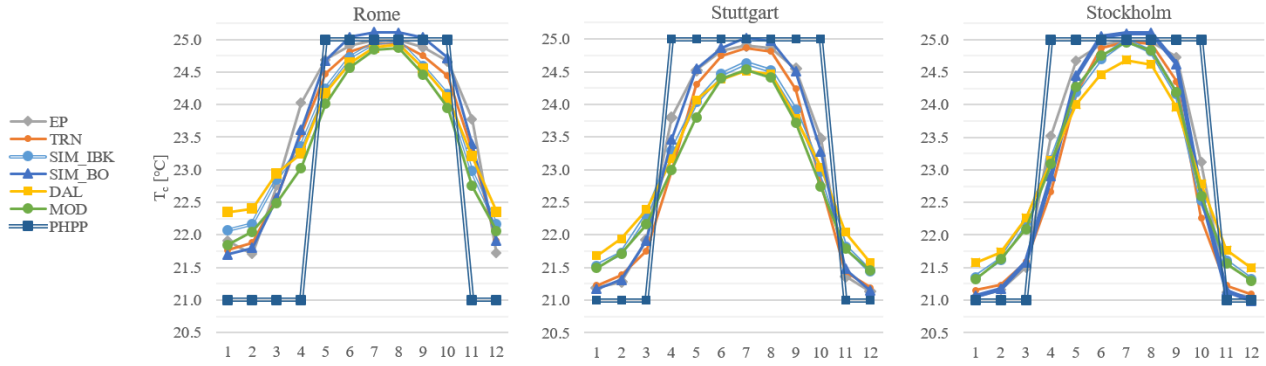

Figure 5: Monthly average of the convective temperature for all the considered tools and climates.

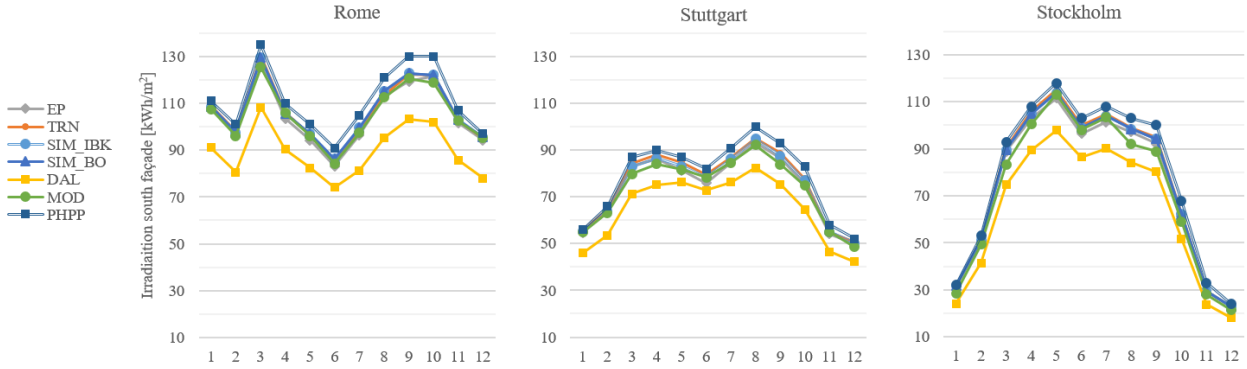

Figure 6: Monthly values of the solar radiation impinging the south façade for all the considered tools and climates.

Figure 7 shows the yearly transmission losses through the wall and windows for each tool in each climate. The wall transmission losses are in the same range in every climate. The median value ranges from -8.2 kWh/(m²a) in Rome to -7.1 kWh/(m²a) in Stuttgart.

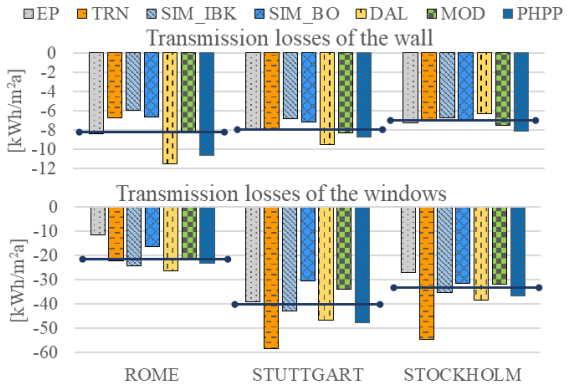

Figure 7: Yearly values of the transmission losses of the walls (top) and windows (bottom).

The deviation of the yearly transmission losses through the wall with respect to the median value (considering the results from EP, TRN, SIM_IBK, SIM_BO and MOD) ranges in Rome from +41% (DAL) to -27% (SIM_IBK), in Stuttgart ranges from +19% (DAL) to -15% (SIM_IBK) and in Stockholm ranges from +15% (PHPP) to -11% (DAL). The transmission losses through the windows are significantly higher than those through the wall and are in the range of 80% of the total transmission losses. The deviation of the windows transmission losses are due to different definitions of the transmission losses, different models of the window and thus different assumptions for the input data.

Influence of the window model

Detailed inputs are required for those tools that use a complex window model (i.e. reflectivity and absorption coefficients for each layer of each pane). The Task56 report (D'Antoni, et al., 2017) describes only the overall glazing system properties defined using a specific set of boundary conditions (i.e. U, g-value, T_{sol}, R_{sol} and T_{vis}, see Table 1). The translation of these overall properties into detailed pane level properties was identified as a source of deviations. In this reference office, the window model plays an important role in the building energy balance of the thermal zone since its properties define the admission of solar gains and 80% of the transmission losses.

To illustrate the influence that user interpretation of overall glazing properties can have on the overall results, four different window system alternatives are tested for the Rome case with EP. The alternatives have similar overall glazing properties but differ in the position and characteristics of the solar control coating, (see Table 9 and Table 10). The window system alternatives are based on measured glass properties from the IGDB.

EP case 1 has the coating placed outside of the inner pane (pos. 3), EP case 2 has the same type of coating placed inside the outer pane (pos. 2) and EP case 3 has an alternative coating in the same position as case 2 which was selected to better match the overall glazing properties, EP case 4 assumes an equivalent layer single pane glazing system with the same overall glazing system properties, under NFRC boundary conditions, as case 3.

Table 10 reports the overall glazing properties and the properties of the coated pane used by EP, TRN, SIM_BO and MOD. TRN, SIM_BO and MOD placed the coating inside the external pane (pos. 2). SIM_BO does not use T_{vis} and T_{sol} because the directly transmitted irradiation is calculated with the overall transmission value of the window.

Table 9: Overall glazing system properties.

Cases	U [W/m²K]	SHGC [-]	T_{vis} [-]	Coating Position
Reference	1.290	0.333	0.659	?
EP: Case 1	1.223	0.359	0.594	Pos. 3
EP: Case 2	1.202	0.326	0.607	Pos. 2
EP: Case 3	1.260	0.350	0.593	Pos. 2
EP: Case 4	1.260	0.350	0.593	Pos. 2
TRN	1.290	0.333	0.659	Pos. 2
SIM_BO	1.290	0.333	0.659	Pos. 2
MOD	1.322	0.334	0.614	Pos. 2

Table 10: Properties of the coated pane.

Cases	Emissivity (coated side) [-]	T_{vis} [-]	T_{sol} [-]
Reference	?	?	?
EP: Case 1	0.021	0.656	0.250
EP: Case 2	0.014	0.673	0.305
EP: Case 3	0.034	0.658	0.269
EP: Case 4	-	-	-
TRN	0.110	-	-
SIM_BO	0.110	-	-
MOD	0.016	0.671	0.310

Table 11 shows the heating and cooling demand of the four variants of the window analysed in EP. Different user interpretations of the overall glazing properties lead to relative deviations, taking as a reference the case 4, in the heating and cooling demand up to 55% and 27%, respectively. The largest deviations can be explained by the position of the solar control coating. With the coating positioned on the inside pane (pos. 3), a smaller fraction of the solar radiation which is reflected and absorbed by the coating, will exit the glazing system on the front side. The overall glazing properties, however, do not represent the angularly dependent nature of the interreflections between the panes well, as can be seen from the deviations of results between cases 3 and 4.

Table 11: Heating and cooling demand for the climate of Rome, with different windows system alternatives.

Cases	Q_h	Q_c	Q_{tr}	Q_{sol}
	[kWh/(m²a)]			
EP case 1	1.6	-46.3	-9.4	28.2
EP case 2	2.5	-39.7	-21.6	32.3
EP case 3	3.6	-36.4	-19.8	25.4
EP case 4	3.4	-40.0	-24.4	33.5
TRN	3.5	-33.3	-29.1	32.9
SIM_BO	3.1	-33.4	-23.1	25.9
MOD	7.1	-34.0	-30.0	31.4

Conclusion

The model of the office cell, reported in IEA SHC Task 56, is implemented by experts in building simulations with different simulation tools (i.e. dynamic tools EnergyPlus, TRNSYS, CarnotUIBK, ALMAbuild, DALEC, Modelica and calculation tool PHPP). The heating and cooling demands, heat losses and gains are investigated considering three different climates (i.e. Rome, Stuttgart and Stockholm). Even when high caution is taken in defining the boundary conditions of a geometrically simple space, user interpretation and implementation in the software remains one of the main reasons for deviations. After several feedback loops, agreement between the experts was achieved to have comparable simulation models implemented. The results, proved to be particularly sensitive to user interpretation of overall glazing system properties. Such deviations amongst tools can be reduced by describing glazing systems using a combination of detailed pane properties as well as overall system properties under varying boundary conditions. A future work will be carried out in order to calibrate the models considering more weather conditions so that they can be used for testing solar passive and solar active façade systems.

Reference

Brange, L., Englund, J., and Lauenburg, P. (2016). Prosumers in district heating networks – A Swedish case study. *Applied Energy 164*, 492-500.

Campana , J., Morini , G., and Magni, M. (2017). The benchmark of the SIMULINK open library ALMABuild for dynamic modelling of buildings. *Proceedings from SET 2017: 16th International Conference on Sustainable Energy Technologies.* Bologna (IT), 17-20 July 2017.

Castaldo, V., and Pisello, A. (2018). Uses of dynamic simulation to predict thermal-energy performance of buildings and districts: a review. *Energy and Environment 7*, 269.

Council of the European Union. (2014). *A policy framework for climate and energy in the period from 2020 to 2030*. Brussels.

Crawley, D. B., Pedersen C. O., Lawrie L. K. and Winkelmann F. C. (2000). EnergyPlus: Energy Simulation Program. *ASHRAE Journal 42*, 49-56.

D'Antoni, M., Bonato, P., Geisler-Moroder, D., Loonen, R., and Ochs, F. (2017). *IEA SHC T56 - System simulation Models Part C Office Buildings*.

Dermentzis, G., Ochs, F., Gustafsson, M., Calabrese, T., Siegele, D., Feist, W., Dipasquale, C., Fedrizzi, R., and Bales, C. (2019). A comprehensive evaluation of a monthly-based energy auditing tool through dynamic simulations, and monitoring in a renovation case study. *Energy & Buildings 183*, 713-726.

Feist, W. (C.F. Müller). (1994). *Thermische Gebäudesimulation: kritische Prüfung unterschiedlicher Modellansätze*. Heidelberg (D).

Feist, W. (2019) *PHPP - Passive House Planning* Package, 1998. Accessed Jan 16, 2019. https://passivehouse.com/04_phpp/04_phpp.htm.

IEA, 2016. International Energy Agency, Solar Heating and Cooling Programme. *IEA SHC Task 56 "Building Integrated Solar Envelope System for HVAC and Lighting".*

ISO 13790 (2008), *Energy Performance of Buildings – Calculation of Energy Use for Space Heating and Cooling* (ISO 13790:2008).

Kim, Y.-J., Yoon, S.-H., and Park, C.-S. (2013). Stochastic comparison between simplified energy calculation anddynamic simulation. *Energy and Buildings 64*, 332-342.

Klein S.A., Beckman W.A., Mitchell J.W., Duffie J.A., Duffie N.A., Freeman T.L., et al., 1979. *TRNSYS 17, TRaNsient SYstem Simulation program*. University of Wisconsin, Madison, WI, USA.

Martinez, R., Goikolea, B., Paya, I., Bonnamy, P., Raji, S., and Lopez, J. (2017). Performance assessment of an unglazed solar thermal collector for envelope retrofitting. *Proceedings from AREQ 2017 International Conference – Alternative and Renewable Energy Quest*. Barcellona (SP), 1-3 Feb 2017.

Pérez-Lombard, L., Ortiz, J., and Pout, C. (2008). A review on buildings energy consumption information. *Energy and Buildings 40*(3), 394-398.

SIA (2015). *Raumnutzungsdaten für die Energie- und Gebäudetechnik* (SIA 2024:2015).

Siegele, D. and Leonardi, E., Ochs, F. (2019) A new MATLAB Simulink Toolbox for Dynamic Building Simulation with B.I.M. and Hardware in the Loop compatibility. *Proceedings from BS 2019: Building Performance Simulation conference*. Rome (IT), 2-4 Sept 2019. Submitted.

Strachan, P., Svehla, K., Heusler, I., ans Kersken, M. (2016). Whole model empirical validation on a full-scale building. *Journal of Building Performance Simulation 9*(4), 331-350.

Werner M., Geisler-Moroder D., Junghans B., Ebert O. and Feist W., 2017. DALEC – A Novel Web-Tool for Integrated Day- and Artificial Light & Energy Calculation. *Journal of Building Performance Simulation 10*(3), 344-363.

Wetter, M., Zuo, W., and Nouidui, S.T. (2011). Modeling of Heat Transfer in Rooms in the Modelica "Buildings" Library. Proceedings of Proceedings from BS 2011: *Building Performance Simulation conference*. Sydney (AUS), 14-16 Nov 2011.

Wetter, M., Zuo, W., Nouidui, S.T., and Pang X. (2014). Modelica Buildings library. *Journal of Building Performance Simulation*, 7:4, 253-270.